Landsat 8 Ice Speed of Antarctica (LISA), Version 1

USER GUIDE

How to Cite These Data

As a condition of using these data, you must include a citation:

Scambos, T., M. Fahnestock, T. Moon, A. Gardner, and M. Klinger. 2019. *Landsat 8 Ice Speed of Antarctica (LISA), Version 1*. [Indicate subset used]. Boulder, Colorado USA. NASA National Snow and Ice Data Center Distributed Active Archive Center. https://doi.org/10.7265/nxpc-e997. [Date Accessed].

Literature Citation

Fahnestock, M., T. Scambos, T. Moon, A. Gardner, T. Haran, and M. Klinger. 2015. Rapid large-area mapping of ice flow using Landsat 8, *Remote Sensing of Environment*. 185. 84-94. https://doi.org/10.1016/j.rse.2015.11.023

FOR QUESTIONS ABOUT THESE DATA, CONTACT NSIDC@NSIDC.ORG

FOR CURRENT INFORMATION, VISIT https://nsidc.org/data/NSIDC-0733

National Snow and Ice Data Center

TABLE OF CONTENTS

1 DATA DESCRIPTION

1.1 Parameters

This data set is a compilation of mean ice flow speed and direction, as well as the estimated uncertainty in these values and the associated data quality parameters.

1.1.1 Sample Data Record

Figure 1 shows an example of ice flow speed from compiled Landsat 8 image pairs for the Filchner Ice Shelf.

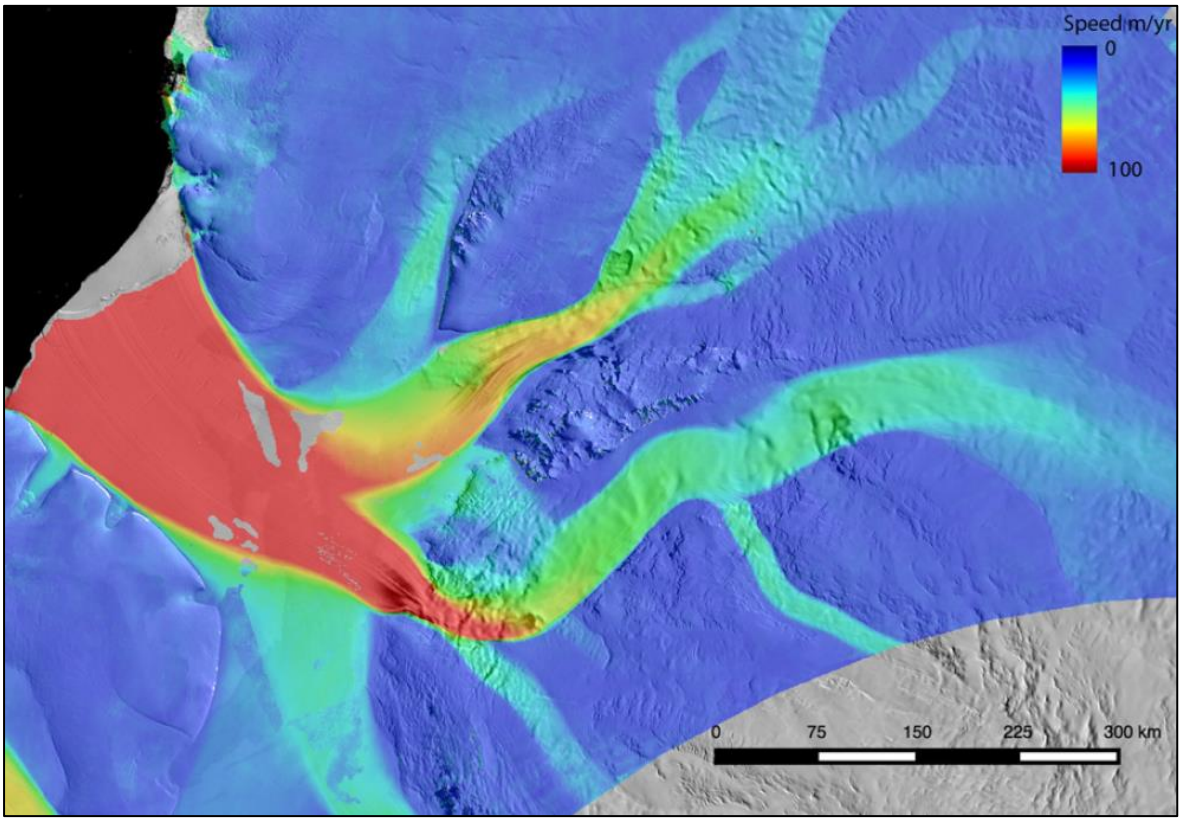

Figure 1. Ice flow speed in m/yr from Landsat 8 for the Filchner Ice Shelf and tributary ice streams. This is an example of the vrgb field, described in detail in Table 1. Ice flow speed is shown in color, superimposed on the MOA2009 image mosaic (Haran et al., 2014). This flow field is a subscene of a continent-wide map using 10,663 image pairs spanning the period from 01 October 2013 to 31 March 2014. For this image, the LISA data were compiled on a nominal 125 m grid to align with the MOA2009 image mosaic.

1.2 File Information

1.2.1 Format

Flow data (`vv, vx, vy`), flow error (`ev, ex, ey`), and data quality (`ct, wt, sd, cr, dc`) files are in 32-bit floating-point GeoTIFF (`.tif`) format. Visualization files (`vrgb, vrgba, varrow`) are 3-band, 8-bit byte GeoTIFF images. Table 1 lists the different data file types provided in this data set.

Table 1. LISA File Types

Category	File Type	Description	Units	Range
Data	`vv`	Surface flow speed at the grid cell (vector sum of x and y)	m/day	0–5.0 m/day
	`vx`	Surface flow speed in x-direction	m/day	0–5.0 m/day
	`vy`	Surface flow speed in y-direction	m/day	0–5.0 m/day
Error	`ev`	Error in speed: standard deviation of all the measurements used for the grid cell	m/day	0–0.5 m/day
	`ex`	Error in speed in x-direction	m/day	0–0.5 m/day
	`ey`	Error in speed in y-direction	m/day	0–0.5 m/day
Data quality	`ct`	Number of image pair velocity measurements that contributed to a grid cell	N/A	0–1119
	`wt`	Mean weight of the velocity mappings used in the composite grid	N/A	0–0.8
	`sd`	Spatial standard deviation: the range of LISA speeds in a 3x3 block of grid cells	m/day	0–0.5 m/day
	`cr`	Mean correlation strength between image pairs that determined the ice displacement for a grid cell	N/A	0–1.0
	`dc`	Mean difference between highest peak and second-highest peak in correlations	N/A	0–1.0
Visualization	`vrgb`	`vv` file rendered in rgb color, overlaid on the MOA2009 image mosaic	m/year	1–3000 m/year
	`vrgba`	`vrgb` file with flow direction arrows (arrow length not scaled to speed)	m/year	1–3000 m/year
	`varrow`	Image of flow direction arrows only	N/A	N/A

1.2.2 Directory Structure

Data are available via FTP in the following directory:

`ftp://ftp.nsidc.org/pub/DATASETS/nsidc0733_landsat_ice_speed_v01/`

The folder /LISA750/ within this directory contains the following six sub-directories:

- `lisa750_2013182_2017120_0000_0400_v01`
- `lisa750_2013182_2017120_0176_0400_v01`
- `lisa750_2013182_2014181_0000_0400_v01`
- `lisa750_2014182_2015181_0000_0400_v01`
- `lisa750_2015182_2016182_0000_0400_v01`
- `lisa750_2016183_2017120_0000_0400_v01`

Each of these sub-directories contains 14 data files in GeoTIFF format.

Note: The first two sub-directories in the list above (`lisa750_2013182_2017120_0000_0400_v01` and `lisa750_2013182_2017120_0176_0400_v01`) contain files spanning the full four-year period, whereas the other four sub-directories contain annual mean files. The difference between `lisa750_2013182_2017120_0000_0400_v01` and `lisa750_2013182_2017120_0176_0400_v01` is the minimum number of separation days (`days_min`); i.e.; `days_min` = 0000 or `days_min` = 0176.

1.2.3 Naming Convention

Example file names:

`lisa750_2013182_2014181_0000_0400_cr_v01.tif`

`lisa750_2016183_2017120_0000_0400_wt_v01.tif`

Data files are named after the following convention and as described in Table 2.

`lisa750_YYYYDDD_yyyyddd_nnnn_NNNN_xx_v01.tif`

Table 2. File Naming Convention

Variable	Description
`lisa750`	Landsat 8 Ice Speed of Antarctica (LISA) 750 m product code
`YYYY`	Four-digit start year (e.g., 2013)

Variable	Description
DDD	Three-digit day of start year (e.g., day 181 of year 2013 = 30 June 2013)
yyyy	Four-digit end year
ddd	Three-digit day of end year
nnnn	days_min: minimum value of separation days used for velocity compositing. Value used in this data set is 0000 or 0176.
NNNN	days_max: maximum value of separation days used for velocity compositing. Value used in this data set is 0400.
xx	File type. See Table 2 for a list of file types.
v01	Version 1
.tif	File format: GeoTIFF

1.2.4 File Size

The data files are approximately 225 MB each; the total file volume is approximately 4.7 GB.

1.3 Spatial Information

1.3.1 Coverage

This data set covers the continent of Antarctica, as described by the polygon vertices listed below and illustrated in Figure 2:

Southernmost Latitude: 90° S
Northernmost Latitude: 60° S
Westernmost Longitude: 180° W
Easternmost Longitude: 180° E

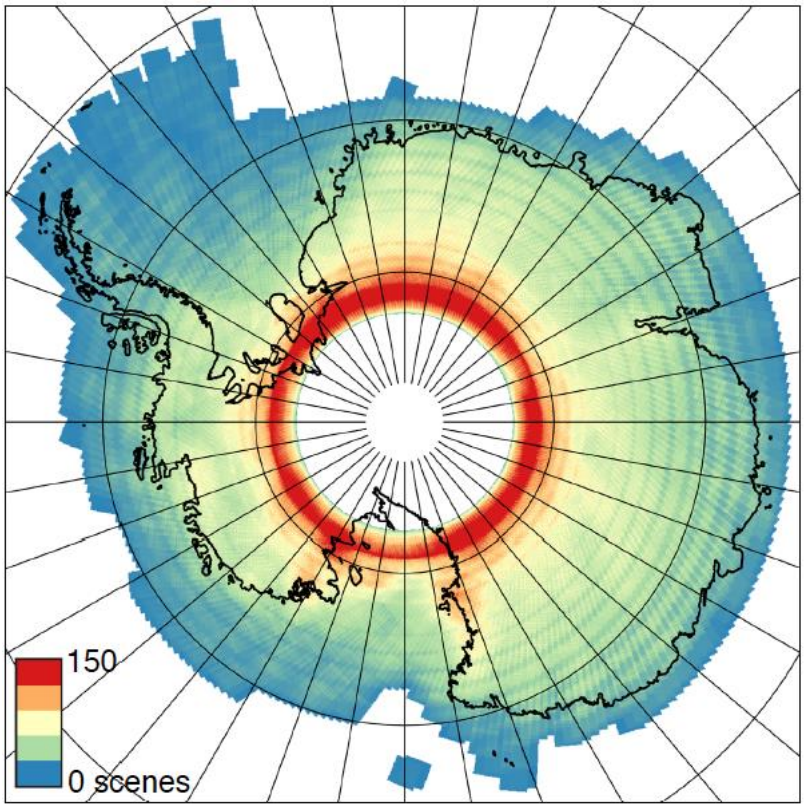

Figure 2. Map of Landsat 8 coverage in Antarctica between 01 October 2014 and 31 March 2015 (Fig. 1a in Fahnestock et al., 2016).

1.3.2 Resolution

The data are gridded at a spatial resolution of 750 m.

1.3.3 Geolocation

The following tables provide information for geolocating this data set.

Table 3. Geolocation Details

Geographic coordinate system	WGS 84
Projected coordinate system	Antarctic Polar Stereographic
Longitude of true origin	0° E
Latitude of true scale	71° S
Scale factor at longitude of true origin	1
Datum	WGS 84
Ellipsoid/spheroid	WGS 84

Units	meters
False easting	0°
False northing	0°
EPSG code	3031
PROJ4 string	+proj=stere +lat_0=-90 +lat_ts=-71 +lon_0=0 +k=1 +x_0=0 +y_0=0 +datum=WGS84 +units=m +no_defs
Reference	https://epsg.io/3031

Table 4. Grid Details

Grid cell size (x, y pixel dimensions)	x: 8056 y: 6964
Number of rows	8056
Number of columns	6964
Nominal gridded resolution	750 m x 750 m
Grid rotation	0° (i.e., 0° longitude at the top of the image)
ulxmap – x-axis map coordinate of the center of the upper-left pixel (XLLCORNER for ASCII data)	-3174450
ulymap – y-axis map coordinate of the center of the upper-left pixel (YLLCORNER for ASCII data)	2406325

Note: The South Pole is not at the center of this grid.

1.4 Temporal Information

1.4.1 Coverages

There are four composited maps with a resolution of one year, covering the following time periods:

- 01 July 2013 to 30 June 2014
- 01 July 2014 to 30 June 2015
- 01 July 2015 to 30 June 2016
- 01 July 2016 to 30 April 2017

In addition, there are two four-year compilations covering the period between 01 July 2013 and 30 April 2017.

1.4.2 Resolution

The temporal resolution of the underlying Landsat 8 image pairs is 16 days. However, the final data product consists only of annual and four-year composited maps.

2 DATA ACQUISITION AND PROCESSING

2.1 Background

The high radiometric resolution and the internal geometric accuracy of the Operational Land Imager (OLI) aboard Landsat 8 enables high-quality ice velocity mapping over ice sheets and large glaciated areas. The 12-bit radiometric quantization and 15-m pixel-scale resolution of the OLI panchromatic imagery allows for displacement tracking of both high-contrast crevasse and debris areas, as well as subtle snow-drift patterns on ice sheet surfaces at roughly 1 m precision (0.1 pixels). Ice sheet and snowfield features typically persist for 16 to 64 days, but can remain for over 400 days, depending primarily on snow accumulation rates and wind erosion. This results in a spatially continuous mapping of ice flow speed, extending the mapping capability beyond crevassed areas (Fahnestock et al., 2016). An early version of the LISA ice velocity data set for the Antarctic ice sheet demonstrated unprecedented coverage across the continent, and provided well-resolved ice flow velocity even at speeds greater than 20 m/yr (Gardner et al., 2018). The data set was part of an assessment of the net ice flux and ice mass balance for the continent.

2.2 Acquisition

Landsat 8 Level-1 terrain-corrected (L-1T) panchromatic band images acquired in 2013 and 2014 were obtained from the USGS. Starting in 2015, data were acquired via Amazon Web Services (AWS) Public Data Sets and Google Earth Engine, although all scenes originate from the USGS Earth Resources Observation and Science (EROS) Center. All descending-node images with less than 50% cloud cover and good panchromatic data (i.e., day-lit scenes) were used in the compilation. The cloud cover information was obtained from the Landsat 8 image metadata.

2.3 Processing

Data were generated using image-to-image correlation software, producing grids of ice displacement referenced to adjacent rock outcrops or using the satellite's geo-positioning information (accurate to ±5 m). This method computes a correlation between two small sub-scenes, or chips, of greyscale data. To map ice flow, chips containing features from one image are compared to a range of possible matching features in a second image. The best match is determined by generating a normalized cross-correlation surface composed of the cross-correlations of chips at each integer pixel offset. Mathematical interpolation of the primary peak in this surface allows determination of feature offset at the sub-pixel level.

The processing steps are outlined in detail below:

2.3.1 High-Pass Spatial Filtering

A Gaussian high pass filter at an approximately 3-pixel scale (50 m) is applied to the original panchromatic band imagery to highlight small-scale patterns of brightness variation. This filtering scheme isolates surface features that are advected with the ice flow, substantially improving displacement retrievals.

2.3.2 Normalized Cross-Correlation

To measure surface displacements, an image-to-image cross-correlation is performed, using a small source chip displaced at integer pixel offsets relative to a larger template chip from a later image. A correlation value is calculated at each offset. The strongest correlation value, or peak of the correlation surface, is then interpolated to estimate the best matching chip offset to the sub-pixel level. The size of the source chips corresponds to 600 m on the ground.

2.3.3 Grid Spacing

Displacement, ice speed, and direction values are posted to an output grid spacing of 300 m (20 pixels) over the common area between the two images. Due to this grid spacing, the pixels used in adjacent chips overlap by 50%, resulting in velocities that are not completely independent measurements of ice flow. However, the result is a smoother and more accurate ice flow map.

2.3.4 Correlation Strength

LISA also includes grids of the peak correlation values (`corr`), the difference between the peak correlation values and the second highest peak in the correlation surface (`del_corr`), and the curvature of the peaks in two dimensions (`d2idx2` and `d2jdx2`). These metrics facilitate the recognition of erroneous matches, such as incorrect peak selection or poorly defined/missing peaks due to noise, and allow for error estimates of each match. In all cases, high values of these quality parameters indicate a more accurate and confident match, whereas lower values indicate uncertainty or error.

2.3.5 Sub-Pixel Offset Determination

Ice sheet and glacier images tend to have a smoothly varying correlation surface in the vicinity of a valid match. To facilitate a more accurate displacement measurement, the algorithm makes use of this tendency by using a bivariate cubic spline to fit the peak in the integer-pixel offset correlation surface and then finding the sub-pixel location of the spline peak. For computational efficiency, a maximum gradient search is performed on the splined surface in the x- and y-directions, locating the peak to within approximately 0.01 pixels.

2.3.6 Masking Single-Pair Velocity Images to Create High-Confidence Vector Grids

The ice flow velocity and ancillary product grids generated from the image pairs, with nominal postings on a 300 m grid, are assembled into mosaics of 750 m gridding (and into 125 m grids in later versions). All of the mosaics available in the LISA data sets are composited from over 100,000 pair-derived velocity grids that cover the selected time range for the continent. However, despite the thresholds that are used in the pair processing, there are spurious or erroneous vectors in the single-pair grids.

Several steps are taken to eliminate erroneous vectors prior to compositing. First, a mask is created on the 300 m vector grid to mask any vectors with del_corr values less than 0.15. For the remaining unmasked vectors, the difference between the ice speed (vv) at the assessed pixel and the eight adjacent ice speeds is examined (i.e., the eight sites surrounding the center pixel in a 3x3 array). These surrounding grid sites may be populated with vectors from the image pair processing run. If the assessed vector doesn't have any adjacent vectors, it is eliminated. If only one other vector exists within the eight adjacent sites, the assessed vector is masked if the difference is greater than 1 m/day. If the assessed vector has two or more neighbors, it is masked unless the assessed vector is within three standard deviations of the adjacent vv values. After these masking steps are applied, the image is tested for all 3x3 regions, and the center pixels from those regions with a standard deviation greater than 1 m/day are eliminated. The single-pair image mask is then applied, and the vector compositing process is continued using the masked vector fields.

2.4 Quality, Errors, and Limitations

Errors in offset determinations result either from cross-correlation inaccurately capturing the pixel offset or from improper correction for the existing geolocation errors between image pairs. Cross-correlation may fail to accurately capture pixel offsets due to: a) signal-to-noise issues, b) pattern repetition in the feature being tracked, or c) the influence of a pattern that is not due to ice motion. An example of the latter is a shift in a ridge line shadow on an east-west trending glacier as the sun changes elevation with the seasons. While it is not possible to mask out all poor matches, it is possible to recognize regions that behave in a spatially consistent manner and that show little offset in non-moving areas. Mitigation strategies for correcting geolocation errors between image pairs depend on the information available for recognizing the issue.

In the case of the Antarctic ice sheet, which has few areas of exposed land surface to constrain the geolocation offsets between image pairs, the determined offsets are compared with rock outcrop areas and slow-moving regions in an ice sheet velocity mosaic. This approach assumes that ice flowing slower than 40 m/yr in the interior of the ice sheet, well away from the coast or exposed land, is not likely to change its flow speed significantly over the course of a year, whereas flow

variability in outlet glaciers may be larger. Several strategies are applied to Antarctic image pairs, depending on the amount and character of the slow-moving ice in areas that had unmasked offset determinations:

- If fewer than 500 ice grid points are slower than 40 m/yr, no offset correction is applied.
- If more than 2000 ice grid points are slower than 40 m/yr, then constant x- and y-offsets are calculated and applied to the x- and y-offsets measured over the whole scene.
- If the majority of ice grid points are slower than 20 m/yr and the above corrections cannot be applied, then the ice is assumed to be stationary and constant x- and y-offsets are calculated and applied to the x- and y-offsets measured over the whole scene.

Rock outcrop areas (assumed to be unmoving) were generated from the Antarctic Digital Data base rock outcrop polygons, dilated by one 300 m pixel to partially eliminate ice-adjacent and mixed ice-rock regions from the 300 m grid. The expected slow-moving regions are derived from an InSAR-based mosaic (Rignot et al., 2011), meaning that the Landsat-generated fields from single pairs were broadly compared to the InSAR velocity field and bulk offsets were applied to the image-pair vector grids before compositing. Note that the Landsat data are more recent and more complete than the original InSAR mapping data. This approach assumes that slow ice flow areas well away from rock exposure are also generally areas of small absolute ice speed change. The Rignot et al. (2011) velocity data are primarily based on measurements from 2006, 2007, and 2008.

2.4.1 Compositing the Mosaics from the Masked Vector Grids

Once the rock and low-velocity corrections have been applied according to the stated rule-based system, the masked 300 m/cell single-pair vector fields are resampled to the target grid spacing of 750 m. Similar tests are applied to the re-sampled vector fields to check for unintended effects of re-gridding.

The re-sampled 750 m single-pair vector grids are then composited in a weighted mean scheme for the available path-row pair data covering a target output grid cell. Weighting of the vectors is based on both the time-separation of the images (lower weights for short separations of 16 to 48 days) and on the basis of the strength of the determined correlation and `del_corr` value for the vector. As the vector grids are composited step-wise one by one, an adapted version of the algorithm of West (1979) was used to build the composite.

To produce the final mosaics, a pole-hole mask extending to 82.75° S is applied, and a correction factor to convert polar-stereographic distances to true distances (and therefore velocities) is used. Finally, ancillary visualization files of flow speed (`vrgb`) and flow direction (`vrgba`) are created.

2.5 Instrumentation

Data were collected by the OLI aboard the Landsat 8 satellite. For more detailed information, visit the NASA Landsat 8 and OLI web pages.

3 SOFTWARE AND TOOLS

The data files in GeoTIFF format may be viewed with ESRI ArcGIS, QGIS, or similar Geographical Information System (GIS) software.

4 RELATED DATA SETS

Global Land Ice Velocity Extraction from Landsat 8 (GoLIVE)
MEaSUREs Annual Antarctic Ice Velocity Maps 2005-2017
MODIS Mosaic of Antarctica 2003-2004 (MOA2004) Image Map
MODIS Mosaic of Antarctica 2008-2009 (MOA2009) Image Map
MEaSUREs MODIS Mosaic of Antarctica 2013-2014 (MOA2014) Image Map

5 RELATED WEBSITES

USGS Landsat 8

6 CONTACTS AND ACKNOWLEDGMENTS

Ted Scambos
University of Colorado, Boulder
NSIDC / CIRES
Boulder CO 80303

6.1 Acknowledgements

This work was supported by NASA Grants NNX14AR77G and NNX15AC70G to M. Fahnestock and NNX10Al42G (supplement) to T. Scambos, as well as USGS Contract G12P00066 to T. Scambos (supporting T. Haran and M. Klinger). T. Moon was supported as a Cooperative Institute for Research in Environmental Science (CIRES) Visiting Post-Doctoral Fellow at the University of Colorado, Boulder, for July 2014 to June 2015. Funding for A. Gardner's effort was supported by NASA's Cryosphere program.

7 REFERENCES

Fahnestock, M., T. Scambos, T. Moon, A. Gardner, T. Haran, and M. Klinger. 2016. Rapid large-area mapping of ice flow using Landsat 8. *Remote Sensing of Environment*. 185: 84–94. doi: https://doi.org/10.1016/j.rse.2015.11.023.

Gardner, A. S., G. Moholdt, T. Scambos, M. Fahnstock, S. Ligtenberg, M. van den Broeke, and J. Nilsson. 2018. Increased West Antarctic and unchanged East Antarctic ice discharge over the last 7 years. *Cryosphere*. 12(2): 521–547. doi: https://doi.org/10.5194/tc-2017-75.

Haran, T., J. Bohlander, T. Scambos, T. Painter, and M. Fahnestock. 2014. MODIS mosaic of Antarctica 2008–2009 (MOA2009) image map. Boulder, Colorado USA: National Snow and Ice Data Center. doi: http://dx.doi.org/10.7265/N5KP8037.

Rignot, E., J. Mouginot, and B. Scheuchl. 2011. Antarctic grounding line mapping from differential satellite radar interferometry. *Geophysical Research Letters*. 38: L10504. doi: https://doi.org/10.1029/2011GL047109.

West, D. H. D. 1979. Updating mean and variance estimates: an improved method. *Communications of the ACM.* 22(9): 532–535. doi: https://doi.org/10.1145/359146.359153.

8 DOCUMENT INFORMATION

8.1 Publication Date

24 May 2018

8.2 Date Last Updated

20 May 2021